8th International Conference
on
Wind Turbine Noise
Lisbon – 12th to 14th June 2019

Long-term noise monitoring of wind turbine amplitude modulation

Christopher Feist, University of Minnesota, St. Anthony Falls Lab: feist020@umn.edu

Matt Lueker, University of Minnesota, St. Anthony Falls Lab: luek0004@umn.edu

William Herb, University of Minnesota, St. Anthony Falls Lab: herb0003@umn.edu

Jeff Marr, University of Minnesota, St. Anthony Falls Lab: marrx003@umn.edu

Peggy Nelson, University of Minnesota, Speech-Language-Hearing Sciences: nelso477@umn.edu

Summary

A noise logging system capable of measuring 100 ms 1/3 octave bands was deployed 600 m north from a 2.5 MW wind turbine at the University of Minnesota's wind energy field research station for one year. The field station includes a 130 m meteorological tower located 170 m south of the turbine, which has wind, temperature, and humidity sensors at six elevations between 7 and 130 m. High-resolution wind speed and turbine SCADA data were recorded in conjunction with the noise measurements. Using these data we investigate correlations between meteorological data, turbine operating conditions, and the presence of amplitude modulation (AM). Analysis of the long-term turbine noise is performed using the IoA (Institute of Acoustics) method for quantifying AM rating.

AM rating was found to have moderate correlation with wind shear exponent, incoming velocity at elevation of 10 m, and turbine power output. The r correlation coefficient is equal to -0.37, 0.44, and 0.65 for the parameters, respectfully. The negative correlation with wind shear is opposite of what researchers have hypothesized to be the cause of enhanced AM and may indicate far-field AM is influenced by the sound propagation path rather than incoming flow conditions for a wind turbine.

1. Introduction

Wind turbine noise has been a significant obstacle to new wind projects in the United States. Wind projects are evaluated prior to installation to verify noise regulations are met, which is intended to reduce noise related annoyance. However, current regulations do not account for the sometimes variable noise characteristic of wind turbines that can cause annoyance even at low sound levels (Pedersen, 2004). This variability in wind turbine generated noise is termed amplitude modulation (AM) and is typically described as a “swishing” or “thumping” noise. The wind turbine sound is amplitude modulated in time by the blade passing frequency (BPF). It has been proposed that there are two types of AM, each having there own mechanisms. Near-field AM, or normal AM, is caused by the directivity of the trailing edge sound produced by wind turbine blade. Oerlemans demonstrated an increase in sound level as the blade moves toward the receptor, and a decrease as the blade moves away (Oerlemans, 2007). This near-field AM is typically observed in the cross-wind directions and at distances of up to 300 m from the wind turbine generator (WTG). At distances greater than a few rotor diameters and in the upwind and downwind directions, normal AM is diminished.

The second type of AM has been termed enhanced AM (EAM). EAM is defined as a variation in sound level that is greater than normal AM and is perceived in the upwind and downwind directions at distances in the far-field, 400 m and greater (Oerlemans, 2013). The mechanism for EAM is not fully understood; however, a number of theories have been presented. Synchronizing of sound between different WTGs (van den Berg, 2004) is one possibility. Oerlemans performed simulations to study the effects of wind shear on sound characteristics of WTG. It was reported that under certain operation conditions, strong wind shear can lead to local stall on a wind turbine blade during the upper part of the revolution. The simulation showed the sound characteristics due to local stall are similar to EAM measured in the field.

Alternatively, studies have shown little correlation between AM rating and meteorological conditions (Bonsma, 2017 and Cand, 2012) and suggest AM might be explained by the sound propagation path to the receiver. Larsson demonstrated wind direction and sound speed gradient are key parameters explaining the occurrence, or probability of occurrence, of AM immission but not emission (Larsson, 2014).

This paper discusses measurements made at a single utility-scale WTG for approximately one year. During the measurement period, acoustical, meteorological, and SCADA measurements were made nearly continuously. WTG sound was measured at a distance of 600 m north of the WTG. Meteorological data were measured at a met tower 170 m south of the WTG. Of primary interest was the observed AM rating at the acoustical measurement location and correlations with meteorological data. The Institute of Acoustics AMWG method is used for rating AM. The paper also investigates meteorological conditions which are most likely to produce AM imission.

2. Field Measurement Site

Field measurements were performed at the University of Minnesota’s Eolos Wind Energy Research Station. A single 2.5 MW Clipper Liberty C96 WTG with a hub height of 80 m and 96 m rotor diameter is operated on the site. The landscape is relatively flat farm land with some groups of trees in the area. Trees were cleared in the predominant wind directions, south and northwest, up to 600 m from the turbine with a width of 300 m centred on the WTG. To the west of the turbine, starting at approximately 200 m from the WTG, are a significant number of trees. A highway is located approximately 1 km to the east of the site and carries moderate traffic.

Due south of the turbine is a research grade meteorological tower with a height of 130 m, spanning the swept area of the WTG blades. Ten elevations between 7 m and 128 m are instrumented with sensors for characterizing the atmospheric boundary layer (ABL).

3. Measurements

3.1 Acoustic measurements

Acoustic measurement were made at a height of 1.5 m using a Brüel & Kjær Noise Logger Type 3659. The noise logger uses a hand-held analyser Type 2250 and outdoor microphone Type 4952 using a free-field ½" microphone and a shield protecting the microphone against the effects of wind, rain, and perching birds. The noise logger was positioned 600 m north of the WTG in a farm field near a small grove. Sound spectra in 1/3-octave band L_{eq} for the frequency range of 6.3 Hz to 20 kHz were measured at 100 ms time intervals. The 1/3-octave band fast L_{eq} were recorded without weighting so that post-processing could be performed on unweighted values as well as A-weighted. The measurements were made continuously from April 24, 2018 to March 8, 2019.

In addition to the 1/3-octave band L_{eq} measurements, instantaneous sound pressure was recorded at 6.6 kHz with 24 bit resolution. These data were recorded to assist in identifying periods of high AM ratings.

The noise logger was deployed with and powered by photovoltaic solar panels and battery combination. Regular site visits were performed to calibrate the microphone and download data.

3.2 SCADA measurements

The WTG operating parameters were measured via the SCADA system simultaneously with the acoustic measurements. Parameters were logged at 1 Hz and time synchronized via GPS with meteorological measurements. Table 1 gives the parameters that are used in the analysis methodology for this paper.

Table 1. SCADA parameters used.

Parameter	Description
P	Wind turbine generator power output [kW]
γ	Nacelle direction w.r.t. north [deg]

3.3 Meteorological measurements

Atmospheric boundary layer (ABL) parameters were collected from the meteorological tower located 170 m south of the WTG. The 130 m high tower has sensors at elevations spanning from 7.3 m to 127.9 m. Table 2 outlines the sensors at each elevation. Campbell Scientific CSAT3 sonic anemometers are located at 4 elevations (9.9, 29.6, 79, and 127.9 m above ground level) which provide three dimensional wind velocity and temperature fluctuations at 20 Hz. Cup anemometers, wind vanes, temperature sensors, and relative-humidity sensors are located at 6 elevations (7.3, 27.1, 51.5, 76.7, 101.5, and 125.9 m) which provide 1 Hz data. The WTG rotor swept area has a bottom elevation of 32 m and top elevation of 128 m. Meteorological measurements span this entire height.

ABL measurements from the met tower are averaged over 10 minute periods. This averaging period corresponds with the 10 minute averaging period for the AM rating algorithm outlined in Section 4. The 10 minute meteorological window coincides with the beginning and end time of the 10 minute AM analysis.

Measurements from the sonic anemometers provide wind speed in all three directions; U_n – wind speed from the north, U_w – wind speed from the west, and U_z – vertical wind speed. All

velocities presented in this paper were measured at 20 Hz. The horizontal wind components are rotated such that U, the instantaneous streamwise velocity, is aligned with the wind direction and V is the instantaneous spanwise velocity component. The instantaneous vertical velocity is defined as W. These rotated wind velocities are used to characterize the ABL. An average velocity for each 10 minute period was calculated and are defined as $\overline{U}$, $\overline{V}$, and $\overline{W}$.

Table 2. Meteorological instruments and measurement heights. WS, wind speed; WD, wind direction; T, temperature; P, atmospheric pressure; RH, relative humidity.

Height [m]	Parameter	Instrument	Rate [Hz]
1	P	Met One 092	1
7.3	T, WS, WD, RH	Met One 083E, Met One 011E, Met One 024A, Met One 083E	1
9.9	U, V, W, T	Campbell Scientific CSAT3	20
27.1	T, WS, WD, RH	Met One 083E, Met One 011E, Met One 024A, Met One 083E	1
29.6	U, V, W, T	Campbell Scientific CSAT3	20
51.5	T, WS, WD, RH	Met One 083E, Thies First Class, Met One 024A, Met One 083E	1
76.7	T, WS, WD, RH	Met One 083E, Thies First Class, Met One 024A, Met One 083E	1
79	U, V, W, T	Campbell Scientific CSAT3	20
101.5	T, WS, WD, RH	Met One 083E, Thies First Class, Met One 024A, Met One 083E	1
125.9	T, WS, WD, RH	Met One 083E, Thies First Class, Met One 024A, Met One 083E	1
127.9	U, V, W, T	Campbell Scientific CSAT3	20

A number of parameters are used to define the ABL for correlation with AM rating. All values are calculated for a 10 min period. Turbulence intensity, TI, is the amount of turbulence in the flow and is defined by

$$TI = \sigma_u / \overline{U}, \tag{1}$$

where σ_u is the standard deviation of U and is calculated for the same 10 min period as $\overline{U}$. Vertical wind shear defines the velocity difference between elevations in a boundary layer. This paper uses the wind shear exponent, α, from the power law equation to define wind shear. The wind shear exponent is determined by solving for α

$$\overline{U}_{128\mathrm{m}} = \overline{U}_{10\mathrm{m}} \left(\frac{128\ \mathrm{m}}{10\ \mathrm{m}} \right)^{\alpha}, \tag{2}$$

where velocity subscripts indicate elevation. Reynolds stress, or the turbulent transport of momentum, is an indicator of the amount of mixing happening in the boundary layer (BL). An unstable boundary layer has larger values of Reynolds stress as compared to a stable BL. The Reynolds stress term for the vertical kinematic eddy flux of U-momentum is defined as

$$\tau_{\mathrm{Reynolds}} = \overline{u'w'}, \tag{3}$$

where the prime values are the turbulent velocity components, or the variation from the mean, and are defined by $u' = U - \overline{U}$ and $w' = W - \overline{W}$. Vertical kinematic eddy heat flux is a term used to quantify the turbulent mixing of heat in the BL and is defined as $\overline{w'\theta'}$ where θ' is the fluctuation of potential temperature from the mean. Negative values of heat flux occur during stable BLs, larger and positive values occur during unstable BLs (Stull, 1988).

4. AM Rating

The method used to quantify AM was proposed by the Institute of Acoustics (IOA) Amplitude Modulation Working Group (AMWG) and is used in this study. The method is designed to identify AM from wind turbine noise and not fluctuations in the background sound level. This is achieved by identifying the blade passing frequency (BPF) in the variation of 100 ms L_{Aeq} over a 10 s period. 10 s periods where no dominant frequency can be identified are rejected. Three frequency bands are analysed, 50 to 200 Hz, 100 to 400 Hz, and 200 to 800 Hz for AM. This paper focuses analysis on the 100 to 400 Hz bandwidth. The resulting series of 10 s AM ratings, which is calculated from the variation in the 100 ms L_{Aeq} over 10 s ($L_5 - L_{95}$), are further processed to identify 10 min windows where AM is identified at least 50% of the time and the 90th percentile of the sequential 10 s AM results is taken. The method produces a series of 10 min AM ratings.

The analysis in this paper uses both the 10 min and 10 s AM ratings for comparison with ABL parameters. The 10 min averaged ABL parameters coincide with 10 min AM ratings. The 10 s AM ratings occur within the start and end time of the ABL parameters, but are not centred in time as that would have significantly increased computational times.

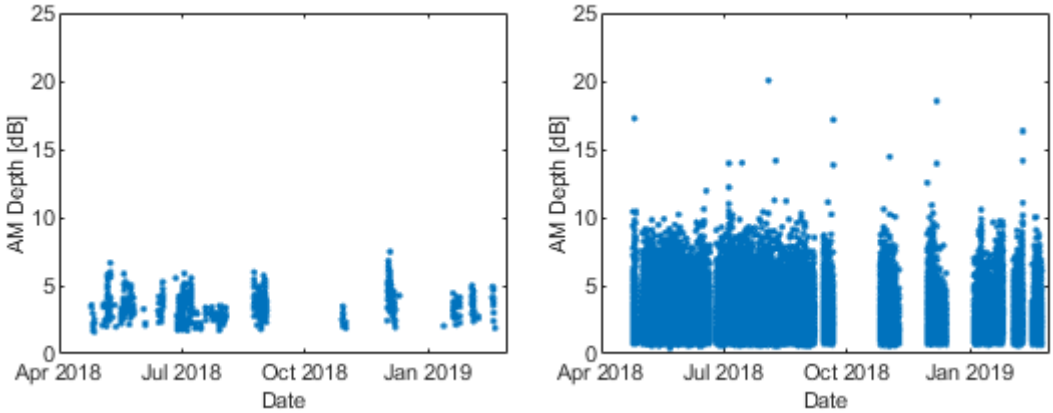

Figure 1. AM modulation rating for 10 min (left) and 10 s (right) analysis

Figure 1 gives the AM rating results for all acoustic measurements from April 24, 2018 to March 8, 2019. Both 10 min and 10 s results are shown, significant AM from the 10 s periods do not meet the criteria for the 10 min AM rating. From the measurement campaign there are 811 ten min periods where AM is identified. The average AM rating is 3.6 dB. There are 43,798 ten min periods between the start and end of measurements where instrumentation was working at the site. This corresponds to identifiable AM occurring 1.85% of the time. Filtering 10 min AM data for wind direction, so that the met tower measurements are not affected by the turbine wake, and instrumentation working leads to 305 ten min AM periods. This is further filtered by looking at data only when the turbine is generating greater than 200 kW, resulting in 183 ten min AM periods. The total number of 10 min ABL measurements is filtered down to 14,918 when the wind direction and turbine power output filters are applied.

5. Results

Measurements are filtered for wind direction such that the met tower is not in the wake of the WTG by filtering out times when wind is +/- 30 deg from due north. This filtering removes conditions where the noise logger is upwind from the turbine which is a limitation on the dataset in this paper. All ABL measurements use this filter unless otherwise stated. Data are further filtered for WTG power production greater than 200 kW for the periods of interest. This paper does not consider the different operating regions of the WTG controller.

Results from correlating ABL parameters with 10 s and 10 min AM ratings are given in Table 3. The reported correlation coefficient, r, uses data where the turbine is operating and generating at least 200 kW over the 10 min period of interest.

Table 3. Correlation coefficients for ABL parameters and AM rating. alpha, wind shear; $\overline{U}_{\mathrm{hub}}$, average hub height streamwise velocity; $\overline{U}_{10\mathrm{m}}$, average streamwise velocity at 10 m; TI, turbulence intensity at 10 m and 128 m; P, turbine output power.

Parameter	r (10 s AM)	r (10 min AM)
α	-0.19	-0.37
$\overline{U}_{\mathrm{hub}}$	0.26	0.40
$\overline{U}_{10\mathrm{m}}$	0.30	0.44
$TI_{10\mathrm{m}}$	0.11	0.08
$TI_{128\mathrm{m}}$	0.15	0.21
$\overline{u'w'}$	-0.20	-0.37
$\overline{w'\theta'}$	0.04	-0.27
P	0.31	0.65

Correlations between ABL parameters and AM rating for the 10 s data, show weak or no correlation. Weak, positive correlations are observed for the streamwise velocity at hub height, $r = 0.26$, and 10 m, $r = 0.30$. Figure 2 is scatter plot where each point is coloured by the spatial density of nearby points as a probability of occurrence in the dataset, termed scatter density plot. The figure shows 10 s AM rating vs hub height velocity (right) and 10 m velocity (left). As the correlation coefficient suggests, velocity at these two elevations are weakly correlated with AM rating as no clear trend can be observed in the scatter. However, the plots show higher probability of AM occurring at lower velocities.

Figure 3 investigates whether this is a phenomenon caused by more data being measured at lower velocities. The plots show the probability distribution of $\overline{U}_{10\mathrm{m}}$ occurring when AM is detected (red) versus during the entire measurement period (blue) for turbine power output greater than 200 kW. Comparing the distributions shows a higher probability of AM occurring at lower 10 m wind velocity as compared to the wind speed distribution for the whole measurement period. Likewise, figure 3 also compares distributions for hub height velocity with AM (blue) and for all measurements. AM is more likely to occur at higher hub height velocities.

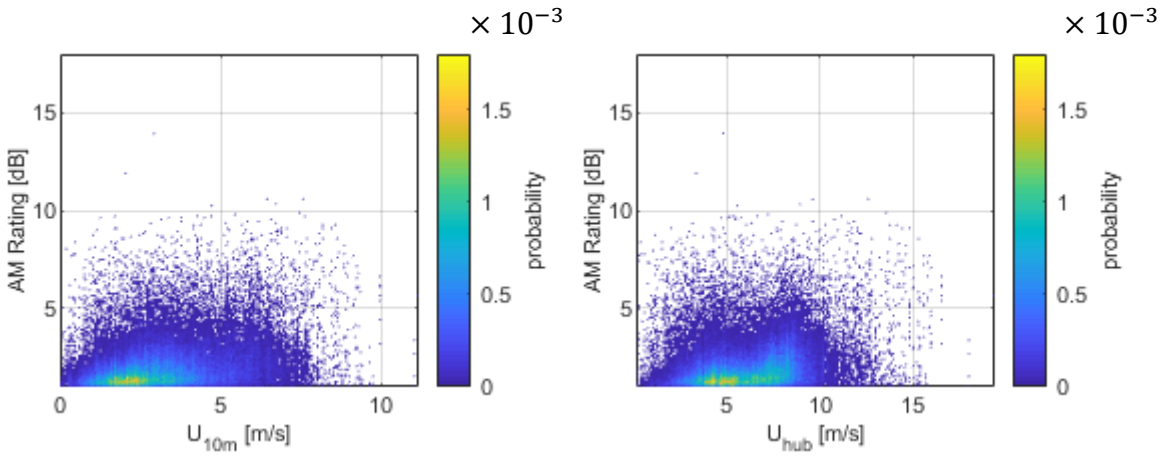

Figure 2. Scatter density plot of $\overline{U}_{10m}$ vs 10 s AM rating (left) and $\overline{U}_{hub}$ vs 10 s AM rating (right).

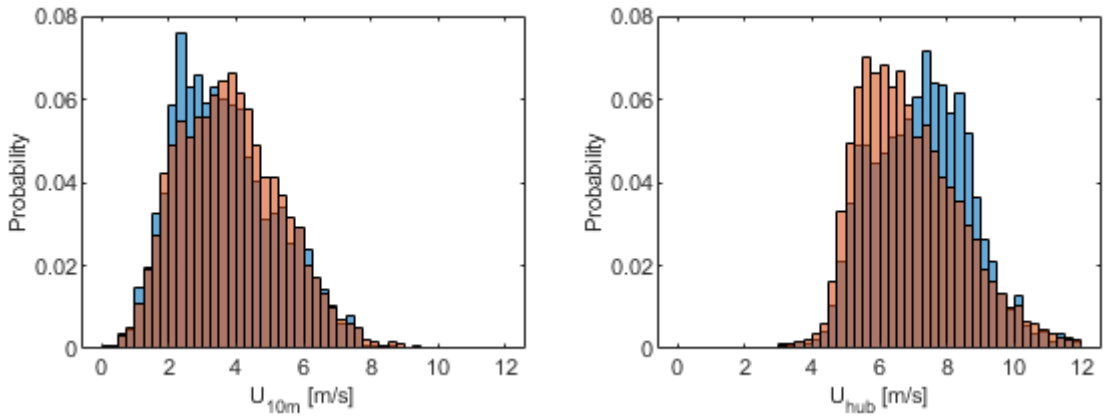

Figure 3. Probability distribution of $\overline{U}_{10m}$ for 10 s AM (blue) and entire measurement period (red). Similarly, probability distribution is shown for $\overline{U}_{hub}$.

The same correlations of velocity at hub height and 10 m are also made with 10 min AM ratings. Here, moderate and positive correlations are found with $r = 0.40$ for $\overline{U}_{\mathrm{hub}}$ and $r = 0.44$ for $\overline{U}_{\mathrm{10m}}$. The stronger correlations are likely a result of less noise in the AM ratings. Figure 4 shows scatter plots of $\overline{U}_{\mathrm{10m}}$ and $\overline{U}_{\mathrm{hub}}$ vs 10 min AM rating. The moderate positive correlation with velocity is seen as a trend in the scatter plot.

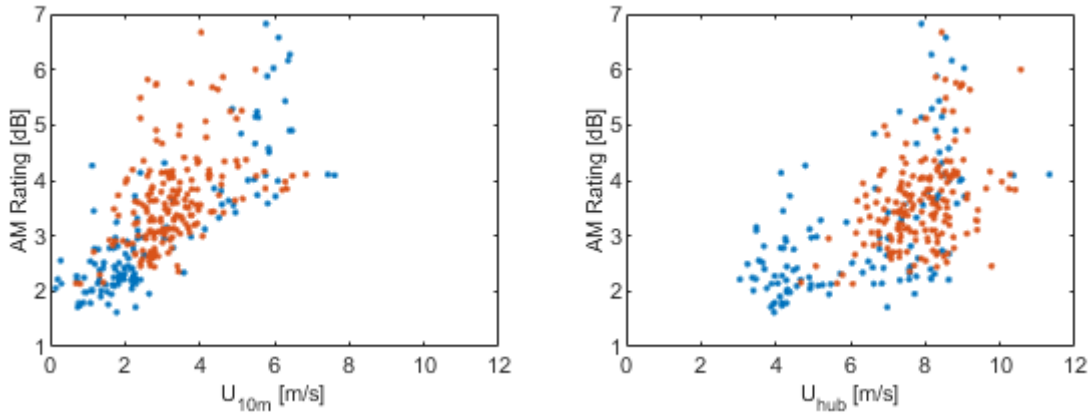

Figure 4. Scatter plot of $\overline{U}_{10m}$ vs 10 min AM rating (left) and $\overline{U}_{hub}$ vs 10 min AM rating (right). Blue points indicate AM ratings where turbine power is ≤ 200 kW, red points turbine power is > 200 kW.

As with the 10 s data, the distribution of hub height and 10 m wind velocities are examined. Figure 5 gives the distribution. The blue histogram is the distribution for wind velocity occurring with 10 min AM, the red histogram is of all (filtered) data from meteorological measurements. Comparing the distributions for $\overline{U}_{\mathrm{10m}}$ shows a difference in probability for 2 – 4 m/s with 10 min AM have a larger probability of occurring for this velocity range. Likewise, $\overline{U}_{\mathrm{hub}}$ in the range of 7 – 9 m/s produces a higher likelihood of AM occurring.

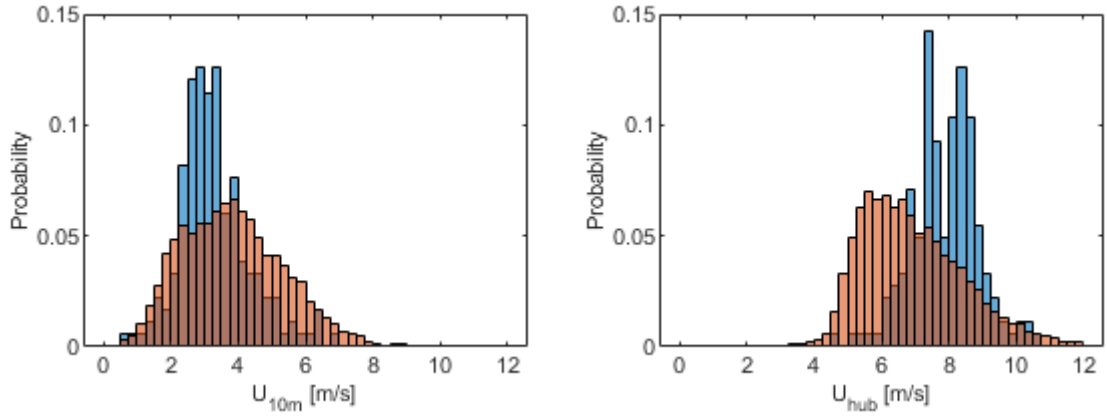

Figure 5. Probability distribution of $\overline{U}_{10m}$ for 10 min AM (blue) and entire measurement period (red). Similarly, probability distribution is shown for $\overline{U}_{hub}$.

Wind shear has been theorized to be a significant factor on the occurrence of AM, where high wind shear during a stable BL creates favourable conditions. i.e. low background noise at the ground due to low wind speeds and wind speed gradient across the WTG rotor, potentially causing partial flow separation at the top of the blade rotation. However, correlation between wind shear exponent and 10 s AM rating found a very weak relationship with r value of -0.19. Figure 6 is scatter density plot of wind shear exponent and turbine power output vs 10 s AM rating. There isn't a clear relationship between wind shear exponent and AM rating, however, higher values of AM occur at lower values of wind shear, or a mixed BL.

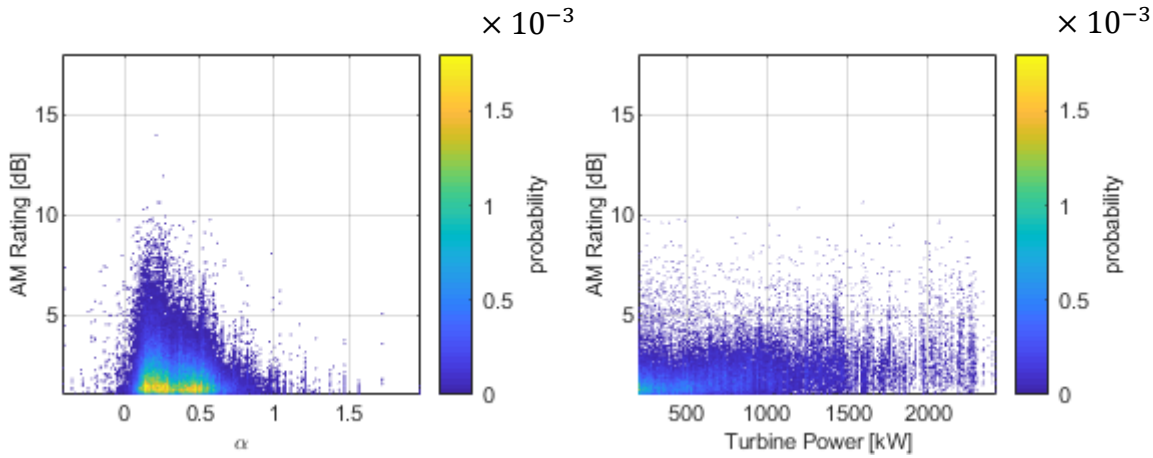

Figure 6. Scatter density plot of α vs 10 s AM rating (left) and turbine power vs 10 s AM rating (right).

Figure 7 shows the probability distribution of wind shear for periods with 10 s AM (blue) and all meteorological measurements (red), the later represents the baseline meteorological conditions for the site. There is a higher probability of AM occurring at larger values of wind shear as compared to the baseline, however, the difference is small at only a few percentage points.

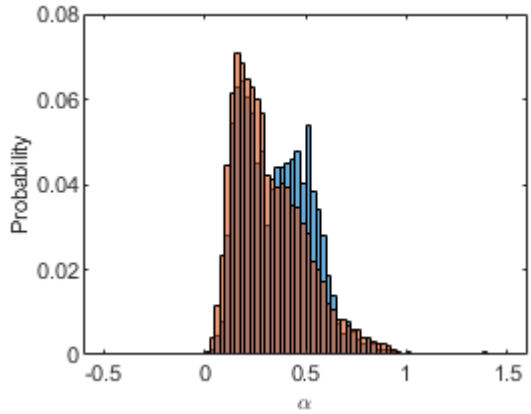

Figure 7. Probability distribution of wind shear exponent for 10 s AM (blue) and entire measurement period (red).

The 10 min AM ratings compared with wind shear exponent shows a stronger relationship as compared to 10 s AM values. A correlation coefficient of -0.37 is calculated. Figure 8 gives a scatter plot of wind shear exponent and turbine power for 10 min AM ratings. The inverse relationship between wind shear and AM rating can be seen. The moderate correlation between turbine power and AM rating is also seen, r value equal to 0.65.

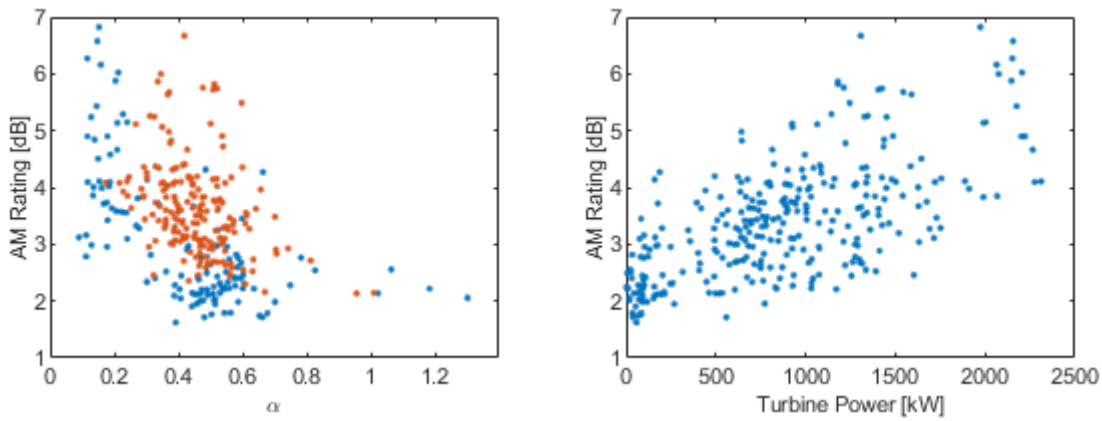

Figure 8. Scatter plot of alpha and turbine power vs 10 min AM rating. Red indicates turbine power > 200 kW.

From figure 8 it appears AM is more densely distributed around higher values of wind shear exponent. This is investigated in figure 9 with a probability density plot of α for periods with 10 min AM (red) and the site baseline condition (blue). Comparing the two distributions we can conclude AM is more likely to occur at higher values of wind shear, or under a stable BL.

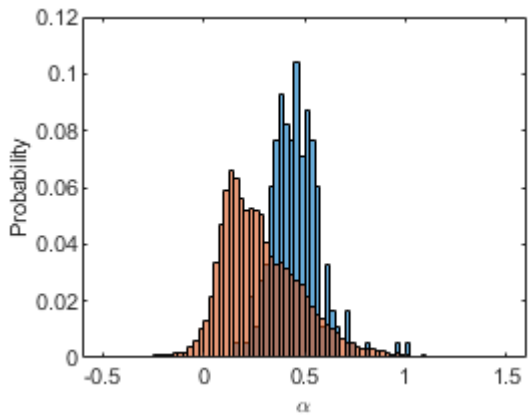

Figure 9. Probability density of wind shear exponent for 10 min AM ratings

Turbulence intensity, heat flux, and vertical momentum flux are also compared against 10 s and 10 min AM ratings. As with the streamwise wind velocity and wind shear exponent parameters, weak or no correlations are made with the AM ratings using the 10 s results. Stronger correlations are typically made with these parameters and the 10 min AM ratings likely due to the 10 min method filtering out contaminated AM ratings with background noise fluctuations.

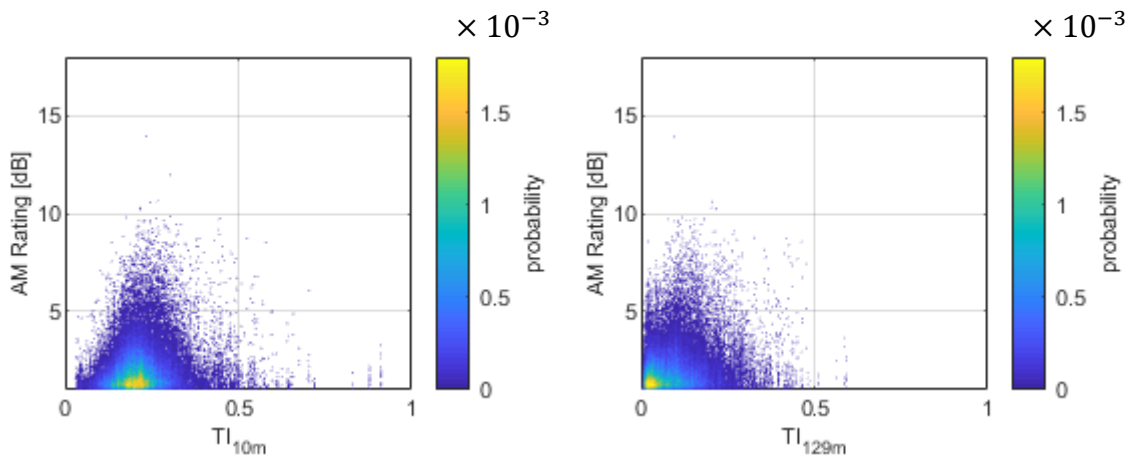

Figure 10. Scatter density plot of turbulence intensity at 10 m and hub height against 10 s AM ratings.

The distribution of the ABL parameter during periods with 10 min AM compared with the site baseline ABL characteristics show values for the ABL parameters at which AM is likely to occur. For example, figure 10 gives scatter density plots for turbulence intensity at 10 m and 129 m vs 10 s AM rating. The distribution of turbulence intensity with AM matches the site turbulence intensity well, figure 11. However, figure 13 shows the higher probability of AM occurring at lower TI values which is indicative of a stable boundary layer. Data used in the distribution of figure 13 are given in figure 12.

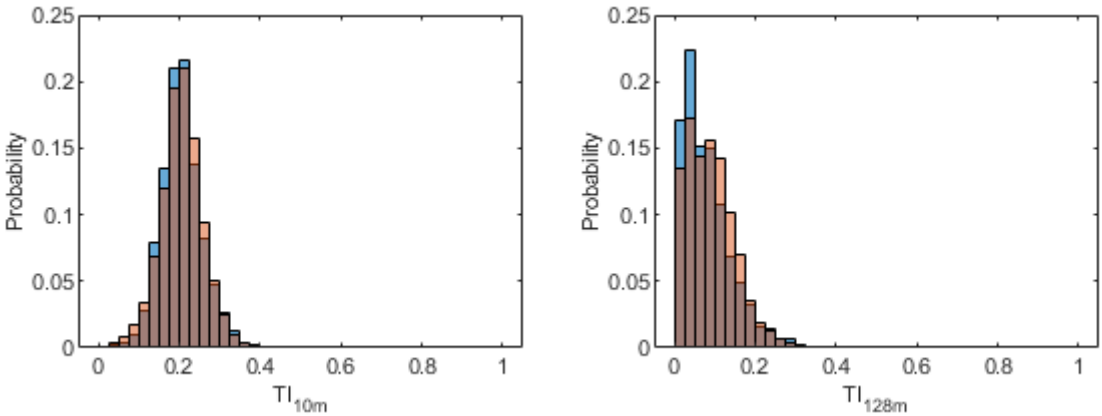

Figure 11. Probability distribution of turbulence intensity for 10 s AM ratings (blue) and baseline site meteorological conditions (red).

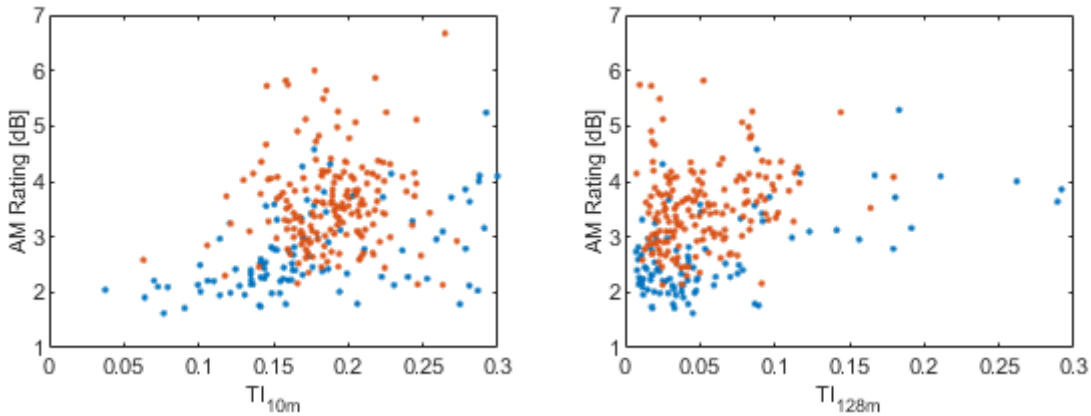

Figure 12. Scatter plot of turbulence intensity vs. 10 min AM rating for 10 m and 128 m elevations. Red indicates turbine power > 200 kW.

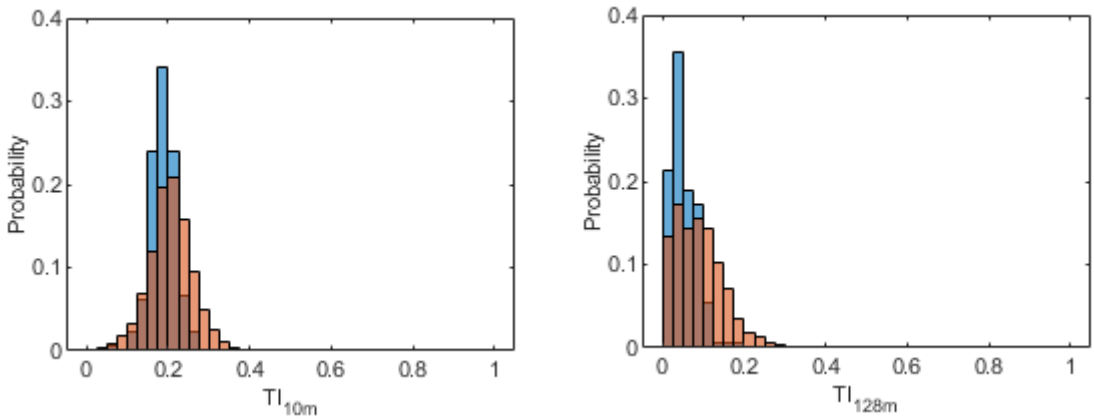

Figure 13. Probability distribution of turbulence intensity for 10 min AM ratings (blue) and baseline site meteorological conditions (red).

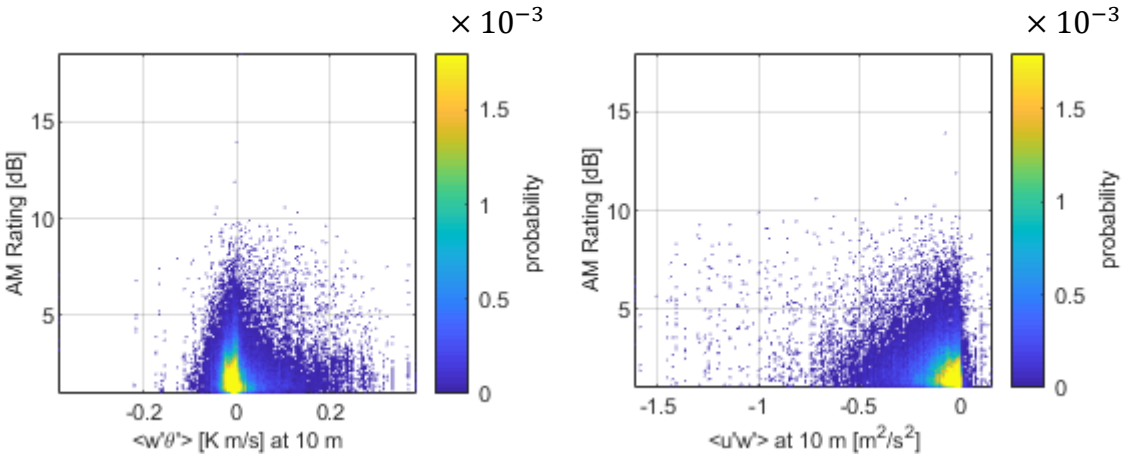

Figure 14. Scatter density plot turbulent heat flux vs 10 s AM ratings (left) and turbulent momentum flux vs 10s AM ratings (right).

The turbulent heat flux parameter, $\overline{w'\theta'}$, is an indicator of the stability of the BL. Negative values indicate a stable boundary layer, positive values an unstable BL. The scatter density plot in figure 14 shows higher values of AM occurring, as well as more often, near turbulent heat flux values around zero. This is confirmed by figure 15 where AM occurs more often at $\overline{w'\theta'} < 0$.

No obvious relationships are seen for $\overline{u'w'}$ in figures 14 and 15.

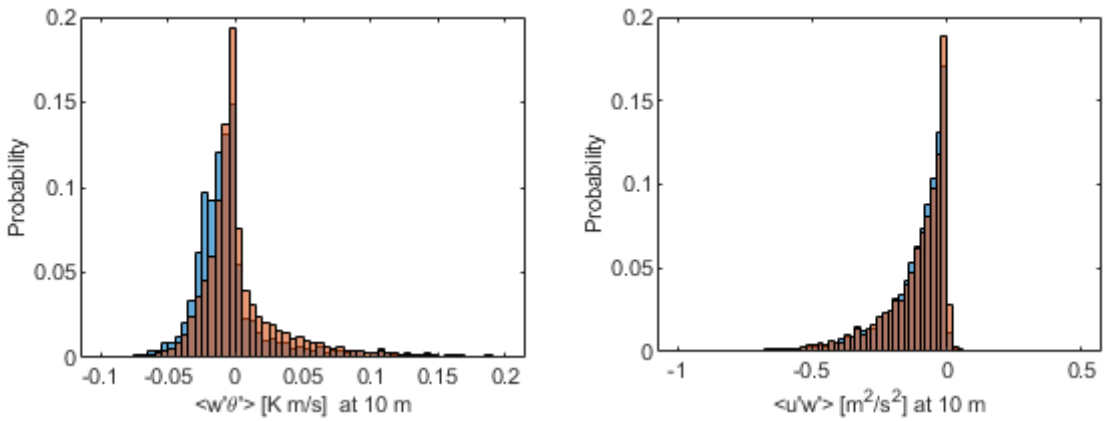

Figure 15. Probability distribution for turbulent heat flux (left) and turbulent momentum flux (right) during 10 s AM shown in blue. Red is the distribution for the site baseline turbulent fluxes.

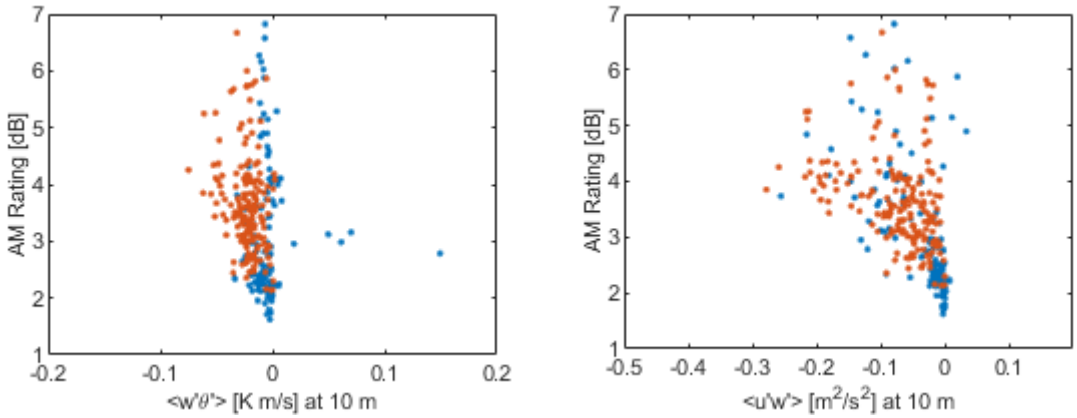

Figure 16. Scatter plot of turbulent heat flux vs. 10 min AM rating (left) and turbulent momentum flux vs 10 min AM rating (right). Red indicates turbine power > 200 kW.

Lastly, turbulent flux parameters are compared with 10 min AM ratings in figure 16. The turbulent heat flux shows a strong relationship between a stable BL, $\overline{w'\theta'} < 0$, and the presence of 10 min AM. This is further seen in figure 17 which shows the distribution of turbulent heat flux with AM vs the site baseline distribution. There is a weak relationship between decreasing heat flux and increasing 10 min AM rating, $r = -0.27$; however this is the only ABL parameter investigated in this study which shows a relationship between a stable BL and increasing levels of AM.

Larger absolute values of turbulent momentum flux, $\overline{u'w'}$, indicate a more turbulent BL. It is not clear at what values a stable BL or unstable BL occur, however, figure 17 indicates AM is more likely to occur at smaller absolute values of $\overline{u'w'}$ which would suggest a stable BL and is consistent with all other ABL parameters.

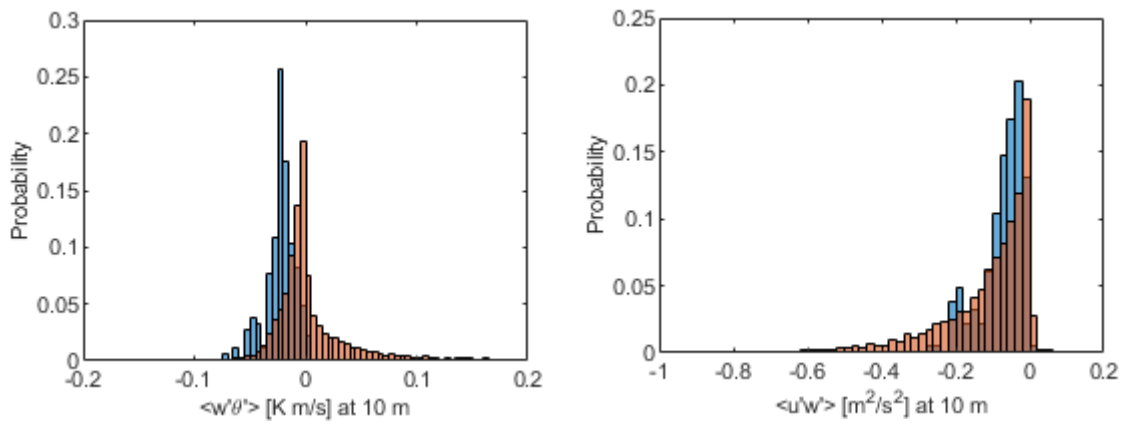

Figure 17. Probability distribution of turbulent fluxes with 10 min AM ratings (blue) and all meteorological measurements.

6. Conclusions

Correlations between ABL parameters and AM rating were investigated over a year-long measurement campaign at a single WTG site. Weak or moderate correlations were made. Wind shear exponent was negatively correlated with AM rating indicating higher values of AM typically occurring during an unstable BL. However, 10 m and hub height streamwise velocity and turbine output power had positive correlations with AM rating which may suggest it is a function of background noise fluctuations at the receiver. Further, the probability distributions for the ABL parameters with AM indicated higher probabilities of AM occurring when the meteorological conditions suggest a stable BL. The only ABL parameter to show correlations between a stable BL and higher levels of AM was the turbulent heat flux parameter.

As no strong correlations between meteorological conditions and AM rating were found, it is likely that AM in the far-field is an immission problem, perhaps amplified by inflow conditions at the source. A stable BL is more likely to produce AM, especially in the downwind direction. The cause may be the refraction of the sound waves down, towards the receiver. Further research would need to be performed to study this phenomenon.

References

AMWG, A. M. (2016). *A Method for Rating Amplitude Modulation in Wind Turbine Noise.* Institute of Acoustics.

Cand, M., Bullmore, A., Smith, M., Von-Hunerbein, S., & Davis, R. (2012, April). *Wind turbine amplitude modulation: research to improve understanding as to its cause & effect*. In Acoustics 2012.

Larsson, C., & Öhlund, O. (2014). *Amplitude modulation of sound from wind turbines under various meteorological conditions*. The Journal of the Acoustical Society of America, 135(1), 67-73.

Oerlemans, S., Sijtsma, P., & López, B. M. (2007). *Location and quantification of noise sources on a wind turbine*. Journal of sound and vibration, 299(4-5), 869-883.

Oerlemans, S., & Schepers, J. G. (2009). Prediction of wind turbine noise and validation against experiment. *International journal of aeroacoustics*, *8*(6), 555-584.

Oerlemans, S. (2013). *An explanation for enhanced amplitude modulation of wind turbine noise*. Wind Turbine Amplitude Modulation: Research to Improve Understanding as to its Cause and Effect. RenewableUK.

Pedersen, E., & Persson Waye, K. (2004). *Perception and annoyance due to wind turbine noise—a dose–response relationship*. The Journal of the Acoustical Society of America, 116(6), 3460-3470.

Stull, R. B. (1988). *An introduction to boundary layer meteorology*. Kluwer Academic Publishers.

Van den Berg, G. P. (2004). *Effects of the wind profile at night on wind turbine sound*. Journal of sound and vibration, 277(4-5), 955-970.